Size-Dependent Waveguide Dispersion in Nanowire Optical Cavities: Slowed Light and Dispersionless Guiding

ARTICLE *in* NANO LETTERS · MAY 2009

Impact Factor: 13.59 · DOI: 10.1021/nl900371r · Source: PubMed

5 AUTHORS, INCLUDING:

Brian Piccione
Princeton Lightwave, Inc.
14 PUBLICATIONS **207** CITATIONS
SEE PROFILE

Ritesh Agarwal
University of Pennsylvania
73 PUBLICATIONS **4,183** CITATIONS
SEE PROFILE

NANO LETTERS

2009
Vol. 9, No. 4
1684-1688

Size-Dependent Waveguide Dispersion in Nanowire Optical Cavities: Slowed Light and Dispersionless Guiding

Lambert K. van Vugt, Bin Zhang, Brian Piccione, Arthur A. Spector, and Ritesh Agarwal*

Department of Materials Science and Engineering, University of Pennsylvania, Philadelphia, Pennsylvania 19104

Received February 4, 2009

ABSTRACT

Fundamental understanding of the size dependence of nanoscale optical confinement in semiconductor nanowire waveguides, as expressed by changes in the dispersion of light, is crucial for the optimal design of nanophotonic devices. Measurements of the dispersion are particularly challenging for nanoscale cavities due to difficulties associated with the in- and out-coupling of light resulting from diffraction effects. We report the strong size dependence of optical dispersion and associated group velocities in subwavelength width ZnSe nanowire waveguide cavities, using a technique based on Fabry-Pérot resonator modes as probes over a wide energy range. Furthermore, we observed subwavelength (λ/9) dispersionless waveguiding and significant slowing of the propagating light by 90% (c/8). These results, in addition to providing insights into nanoscale optical transport, will facilitate the rational design of nanowire photonic devices with tailored dispersion and group velocities.

Central to the appeal of utilizing semiconductor nanowires for nanophotonic applications is their ability to confine and guide light at the nanoscale, enabling functionalities such as optical transport,[1,2] resonators,[3] lasers,[4] and sensors.[5] By virtue of the high refractive index mismatch with their surroundings, semiconductor nanowires of subwavelength width strongly confine optical waves and are ideally suited for the development of integrated nanophotonic systems.[6,7] The various confined optical modes propagating in dielectric nanowire waveguides are characterized by their energy-wavevector dispersion, which theory predicts to be strongly size dependent at the nanoscale.[8] Knowledge of the size dependence of the waveguide mode dispersion is crucial for understanding the fundamental size effects of strong optical confinement and the optimal design of nanowire-based photonic devices where a specific dispersion and/or group velocity dispersion may be required. For instance, in optical communication high-speed transmission with a low group velocity dispersion is desirable in order to preserve signal pulse shapes[9] whereas slowed light would, due to increased interaction times and increased electromagnetic energy densities, be advantageous in optical nonlinearity based applications[10] or optical sensing.[11]

While the theoretical mode properties of dielectric (nano)fiber waveguides have been elaborately treated,[6,8,12,13] no experimental data on the size dependence of the waveguide dispersion of subwavelength dielectric nanowires have been reported. Direct measurements of the energy-wavevector dispersion are commonly performed by angle-resolved transmission or emission experiments,[14,15] and time-resolved transmission experiments can measure its derivative, the group velocity.[16] However, for nanowires these measurements are hindered by the scrambling effect of the subwavelength apertures at the wire ends due to diffraction,[17] the short transmission times involved,[10] and the difficulty of in-coupling of the probe light with a large energy and wavevector distribution.[18]

In this Letter we report on the experimentally determined strong size dependence of optical dispersion and associated group velocities in subwavelength width ZnSe nanowire waveguide cavities, using Fabry-Pérot resonator modes as probes over a wide energy range. Furthermore, we observed subwavelength (λ/9) dispersionless waveguiding and significant slowing of the propagating light by 90% (c/8). These results, in addition to providing insights into nanoscale optical transport, will facilitate the rational design of nanophotonic devices with dispersion and group velocity tailored toward specific functions including optical computation,[19] sensing,[11] and communication.[9]

ZnSe nanowires were obtained by the vapor−liquid−solid method using evaporation of elemental precursors and 5 nm Au/Pd covered silicon substrates (for details see the Supporting Information). After synthesis, the nanowires were transferred to Si substrates covered with a 300 nm thermal oxide by dry transfer. The measurement substrates were

* Corresponding author, riteshag@seas.upenn.edu.

10.1021/nl900371r CCC: $40.75
Published on Web 03/05/2009

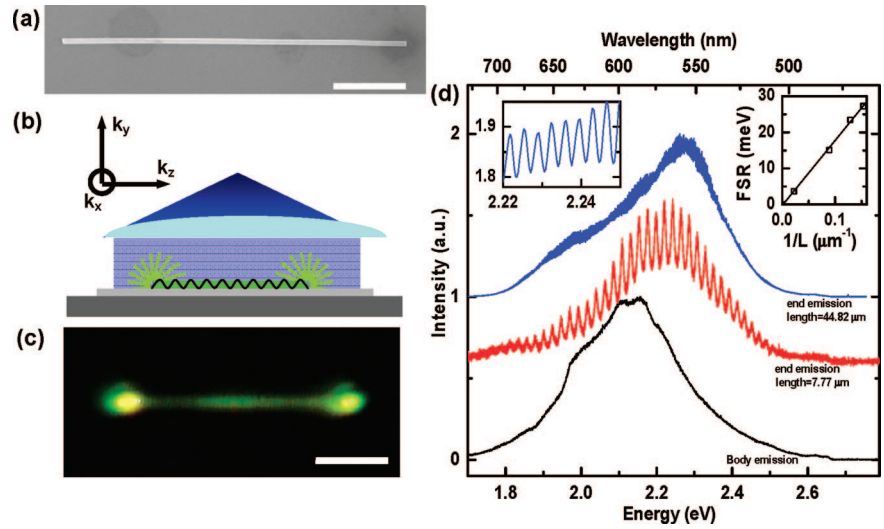

Figure 1. (a) Scanning electron microscopy image of an a ZnSe nanowire dispersed onto a 300 nm thick SiO_2 covered Si wafer. Scale bar, 2 μm. (b) Experimental geometry whereby the nanowire is uniformly excited perpendicular to its long axis. (c) Real color optical image of the emission of a ZnSe nanowire under uniform laser illumination. Scale bar, 2 μm. (d) Typical emission spectra collected at the middle part of the nanowire (lower trace, black), from the end of a 7.77 μm short nanowire (middle trace, red), and at the end of a 44.82 μm long wire (upper trace, blue) show Fabry−Perot modes of the nanowire resonator. A magnification of the upper trace is shown in the left inset. (Right inset) mode spacing at 2.1 eV for nanowires of comparable widths as a function of their reciprocal length, fitted by a least-squares linear fit.

lithographically patterned to contain markers so that individual wires could be characterized by both electron and optical microscopy (Figure 1a). Optical experiments were carried out using a home-built microscope equipped with a Nikon 60× 0.7 NA objective. The 457.9 nm laser line of an argon ion laser (Coherent) provided excitation into the ZnSe conduction band continuum and was focused onto the back aperture of the objective using a beam expander/spatial filter to enlarge to excitation spot to around 1 mm, giving an average excitation power density of 4 W/cm^2. The experimental geometry is shown in Figure 1b. Photoluminescence from the individual wires was collected by the same objective and split off using a dichroic mirror and laser blocking filter. The magnified sample image was projected onto either a small CCD for color imaging or the focal plane of an optical fiber fitted with a focusing lens. When the optical fiber was moved through the image plane using piezo translators (Physik Instrumente), light could be collected from specific parts of the nanowire with a spatial resolution of ~500 nm. The light collected by the fiber was coupled to a 0.5 m spectrometer (Acton), dispersed by a 300 grooves/mm 500 nm blaze grating and detected by a cooled 2048 horizontal pixel CCD (Princeton Instruments) resulting in a full width at half-maximum (fwhm) wavelength resolution of 0.1 nm. After the optical measurements, the lengths (±20 nm) and widths (±4 nm) of the nanowires were determined by scanning electron microscopy (FEI Strata DB235 FIB) with the widest part of the wire taken as the width (diameter), i.e., ignoring any faceting.

A photoluminescence image of a nanowire (Figure 1c) shows, in addition to emission from the nanowire body, pronounced emission from the end facets. Further investigation of the nature of the body and end emission by spatially resolving the spectra shows that the emission from the nanowire body (Figure 1d, black trace) consists of a broad peak centered at 2.15 eV in addition to minor band-edge emission centered at 2.65 eV, characteristic of ZnSe defect emission caused by interstitial Zn ions and exciton recombination, respectively.[20] The emission spectra obtained from the nanowire ends however show a pronounced modulation over a wide spectral range (Figure 1d, red and blue traces), with the modulation period inversely proportional to nanowire length (Figure 1d, right inset) demonstrating that the nanowire functions as an optical Fabry−Pérot resonator along its length. The internally generated light is confined due to the large refractive index mismatch between the nanowire and its surroundings and is waveguided to the ends where it is partially reflected. If the reflection at the ends of the nanowire is sufficiently high and the losses along the length of the wire are sufficiently low, standing optical waves can develop, giving rise to interference peaks in the spectrum of the leaked light at the nanowire ends. In wavevector space these interference peaks are equally spaced at integral multiples of π/L_z (L_z, wire length).[21] Thus, when the peak positions in the energy space are plotted versus incremental wavevector multiples of π/L_z, the shape of the energy-wavevector dispersion can be determined. Since our measurements are obtained in the far-field, the absolute values of the parallel wavevectors cannot be determined. However, by comparison with theoretical calculations based on the numerical solutions of the Maxwell's equations for the measured nanowire size (see Supporting Information), precise assignment of the absolute parallel wavevectors and the waveguided mode type (e.g., hybrid electric, tranverse electric) can be made, which also helps to identify novel nanowire dispersion features owing to their small diameters.

In order to examine the influence of the nanowire width on the mode dispersion, emission spectra were taken from the ends of nanowires with varying width as determined by scaning electron microscopy (SEM) (Figure 2a). Figure 2b

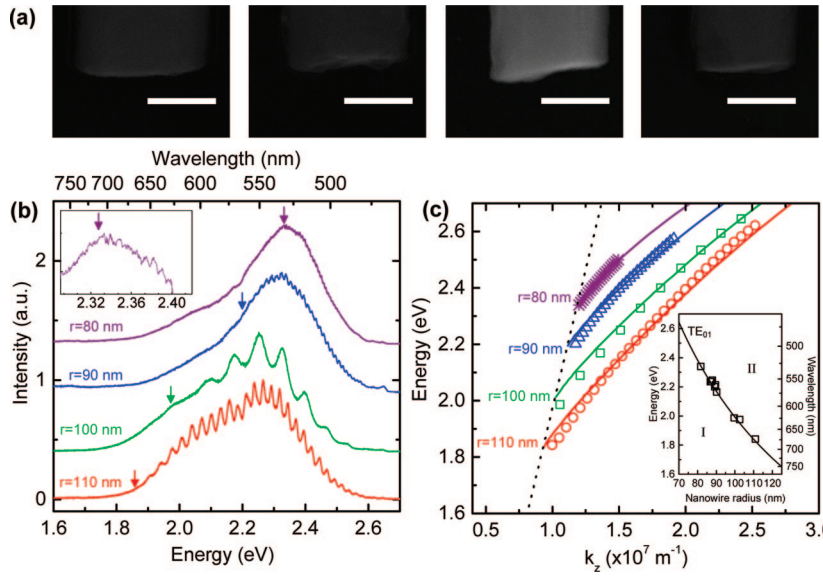

Figure 2. (a) SEM images of four ZnSe nanowires having radii of 110, 100, 90, and 80 nm and lengths of 5.98, 2.08, 11.51, and 22.28 μm respectively (left to right). Scale bars are 100 nm. (b) Emission spectra acquired from the ends of these wires with increasing thickness from top to bottom trace. The inset shows a magnification of the emission spectrum of the thinnest wire (radius 80 nm) in the 2.30−2.40 eV spectral range. The arrows indicate the mode cutoff. (c) Dispersion of the TE_{01} mode of the nanowires with a radius of 110 nm (circles), 100 nm (squares), 90 nm (triangles), and 80 nm (asterisks). The solid lines are the numerical solutions for the eigenvalue equation of the TE_{01} mode of a dielectric cylinder and the dashed line is the dispersion of light in vacuum. In the inset the measured size dependence of the TE_{01} mode cutoff is shown for measurements performed on many more wires with the solid line the result of the calculations (see Supporting Information).

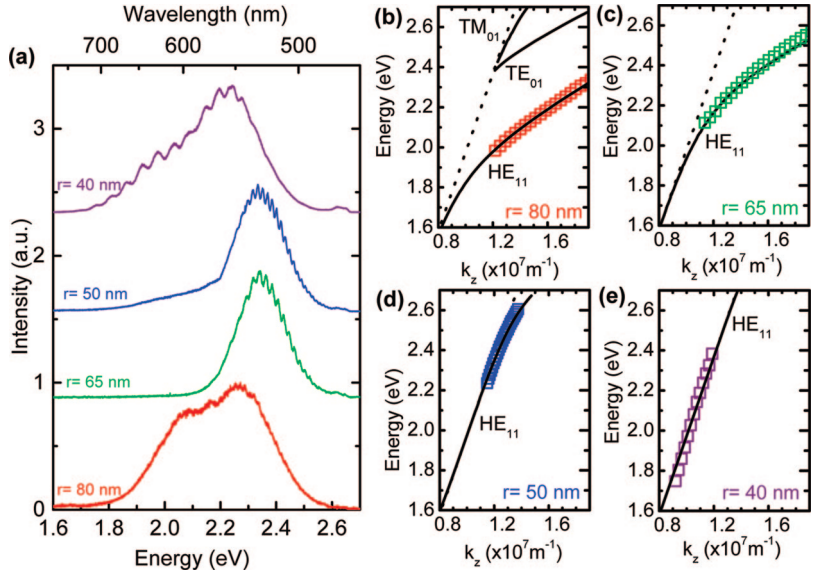

Figure 3. (a) Emission spectra acquired from the ends of nanowires with radii of 75, 65, 50, and 40 nm and lengths of 8.52, 8.02, 33.15, and 14.01 μm, respectively, with increasing thickness from top to bottom trace. (b−e) Dispersion of the HE_{11} mode of the nanowires with a radius of 75, 65, 50, and 40 nm, respectively. The solid lines are the results of the numerical solutions for the eigenvalue equation of the HE_{11} mode of a dielectric cylinder and the dashed line is the dispersion of light in vacuum. In panels d and e the mode dispersion overlaps with the dispersion of light in vacuum.

shows the spectra of these wires with radii of 110, 100, 90, and 80 nm. Aside from the different interference peak spacings caused by the different wire lengths, the spectra show a decrease in the modulation intensity toward lower energy, eventually leading to smooth and unmodulated spectra. This low-energy cutoff, as is indicated by arrows, shifts to higher energy with a decrease of the nanowire width. A plot of the measured interference peaks as a function of incremental wavevector steps for the four different nanowires of different thickness is shown in Figure 2c. The solid lines represent the solutions of the numerically solved eigenvalue equation of an air-clad dielectric cylinder waveguide[8] with the measured nanowire radius and the energy-dependent refractive index as determined from a bulk ZnSe crystal,[22] as input parameters (see Supporting Information). The nanowire width dependence of the measured mode dispersion and their cutoffs corresponds well with the lowest order mode possessing a cutoff, the transverse electric TE_{01} mode. In

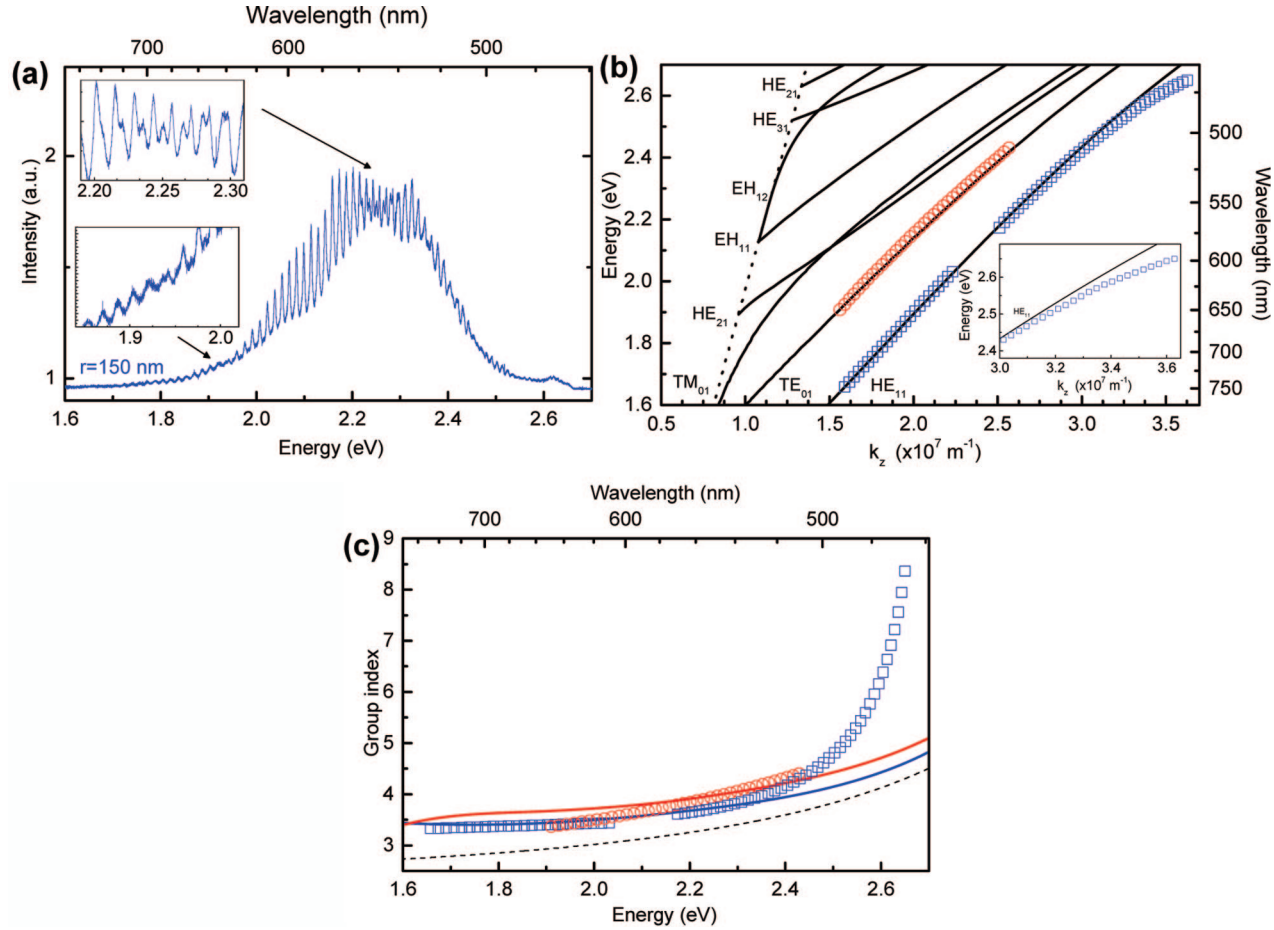

Figure 4. (a) Emission spectrum acquired from the end of a nanowire with a radius of 150 nm. This spectrum shows three series of peaks which can be identified due to their spectral overlap giving rise to irregular periodicity (shown in the insets). (b) Mode dispersion obtained from the spectrum shown in panel a. The solid lines are the results of the numerical solutions for the eigenvalue equation of the modes of a dielectric cylinder and the dashed line is the dispersion of light in vacuum. Inset: Energy-wavevector dispersion close to the band gap region. Close to the band edge of ZnSe (2.69 eV)[22] a strong deviation of the experimental points from the calculations can be seen. (c) Group index obtained by differentiating the mode dispersions in panel b. Experimentally measured group index of HE_{11} (blue squares) and TE_{01} (red circles) modes along with the numerical calculation results based on cylindrical waveguide modes (HE_{11} solid blue line; TE_{01} solid red line). The dashed line represents the group index in a bulk ZnSe crystal.[22] Close to the band edge a pronounced slowing of the light can be seen for the HE_{11} mode.

the inset of Figure 2c the measured TE_{01} mode cutoffs as a function of nanowire width, and hence the boundary between multimode and single mode guiding (indicated by II and I, respectively) are plotted along with the results of the calculations. The good correspondence of the experimental points with the results of the calculations shows that although the nanowires are of subwavelength widths, classical electromagnetic theory can be used to predict the dispersion properties. These results also clearly demonstrate that an increase in the confinement of optical waves leads to a systematic increase in the energy of the energy-wavevector dispersions and the cutoff frequency, analogous to electron waves in quantum-confined nanostructures but explained by purely classical optical wave phenomena.

We further investigated the nanowires in the reduced size regime where only the lowest order, single HE_{11} mode can be guided with no "theoretical" cutoff limit in order to study their size dependence and to determine the longest wavelength that can be guided in the "practical" limit. The spectra obtained from the ends of nanowires with radii ranging from 75 to 40 nm (Figure 3a) show no low-energy cutoffs, in accordance with the theoretical predictions for the lowest order HE_{11} mode.[8] Plots of the Fabry−Pérot mode energy maxima as a function of incremental wavevectors (Figures 3b−d) along with the solutions of the aforementioned eigenvalue equations show excellent agreement and demonstrate that in this size regime the dispersion is highly sensitive to nanowire width. For instance, the wire with a radius of 65 nm shows dispersion more similar to that of bulk ZnSe whereas the wire with a radius of 50 nm shows dispersion more similar to that of the air cladding. For the smallest wire (radius of 40 nm) we find that the dispersion totally coincides with that of light in vacuum; i.e., the light propagates with a group and phase velocity equal to that of light in air. This can be understood by considering that a significant portion of optical waves in the wavelength range of 730−540 nm travels outside of the 40 nm radius nanowire, in the air cladding. It is however surprising that this light is still bound within the nanowire to complete at least one full round trip along the 14.01 μm long wire to display the

Fabry−Pérot modes with a reasonably high quality factor of ∼100, suggesting sufficient mode confinement. This intriguing result shows that nanowires of extremely small widths ($\lambda/9$) can still guide light, without dispersion, which can be very useful for evanescent-wave optical sensors.

We also studied relatively thicker nanowires, which can guide multiple modes simultaneously. The emission spectrum obtained from the end of a 150 nm radius nanowire shows intense Fabry−Pérot modulations (Figure 4a), which upon closer inspection (Figure 4a, inset) display an irregular peak spacing suggesting that at least two sets of modes participate in the standing wave formation. The energy-wavector dispersion of this nanowire (Figure 4b) together with the calculation results show that the spectrum is dominated by the HE_{11} and TE_{01} modes, and not by TM_{01} mode, due to its poor reflectivity.[12] The calculated dispersion shows that in our observation range there is no low energy cutoff for these modes, which is corroborated by the observation of interference peaks down to the lowest observed emission energies. Interestingly, this thicker wire allows us to observe interference peaks up to close to the band gap (2.69 eV at room temperature).[22] It can be seen (Figure 4b and inset) that at energies approaching the band gap of ZnSe, the experimental data deviate strongly from the calculated HE_{11} dispersion. This effect is more clearly seen in Figure 4c where the group index (group velocity normalized to the light speed) of these modes is plotted as a function of emission energy. It can be seen that at low energies (sub band gap) the group velocity is reduced by 35% for the two guided modes with respect to bulk ZnSe (Figure 4c, dotted line), solely due to the lateral confinement of the photon modes. However, more significant effects are observed close to the ZnSe band-edge (2.6 eV) where the group velocity reaches a value of $c/8$, which is clearly not predicted by the calculations. Due to the ZnSe exciton binding energy of 19 meV[22] and the small observed exciton related luminescence peak, we expect that close to the band gap strong light−matter coupling between excitons and photons can occur,[23] resulting in a flattening of the dispersion and hence slowing of light (Figure 4b,c).[16] This effect for macroscopic crystals is already included in the calculations by means of the dispersion of the refractive index which takes into account excitonic contributions.[22] The strength of light−matter coupling in microcavity structures depends on the ratio of the oscillator strength to the optical mode volume.[24] In nanowires it is not unreasonable to assume that the mode volume is considerably reduced compared to larger crystals therefore giving rise to enhanced light−matter interaction as a result of the higher electric field intensities inside the wire, which also agrees with earlier observations in ZnO nanowires.[25] More detailed experiments are currently being performed to quantify the strength of light−matter interaction in nanowire cavities.

In conclusion, we have demonstrated strong size-dependent optical dispersion and group velocities in subwavelength ZnSe nanowire waveguide cavities using Fabry−Pérot resonator modes as probes. The measured dispersions show good correspondence with the calculations for an air-clad dielectric ZnSe cylinder where deviations from cylindrical morphology of the nanowire, substrate interaction, and crystal anisotropy do not have significant effects. Furthermore, we observed subwavelength ($\lambda/9$) dispersionless guiding in the sub-band-gap range and significant slowing of the propagating light by 90% ($c/8$) due to enhanced light−matter interaction close to the exciton resonance. These results open the way to a rational design of semiconductor nanowire photonic devices in which the dispersion and signal speed can be tailored to specific functions, such as enhanced nonlinear effects for optical switching and computing, high-speed, near-dispersionless transmission of optical signals, and enhanced surface propagating waves for evanescent-wave sensor applications.

Acknowledgment. L.K.v.V. acknowledges funding by The Netherlands Organization for Scientific Research (NWO) under the Rubicon programme. This work was supported by the NSF-CAREER award (ECS-0644737).

Supporting Information Available: Details on the ZnSe nanowire growth and the numerical calculations of the propagation constants of ZnSe cylinder waveguides. This material is available free of charge via the Internet at http://pubs.acs.org.

References

(1) Law, M.; Sirbuly, D. J.; Johnson, J. C.; Goldberger, J.; Saykally, R. J.; Yang, P. *Science* **2004**, *305*, 1269.
(2) Barrelet, C. J.; Greytak, A. B.; Lieber, C. M. *Nano Lett.* **2004**, *4*, 1981.
(3) Johnson, J. C.; Yan, H.; Yang, P.; Saykally, R. J. *J. Phys. Chem. B* **2003**, *107*, 8816.
(4) Duan, X.; Huang, Y.; Agarwal, R.; Lieber, C. M. *Nature (London)* **2003**, *421*, 241.
(5) Sirbuly, D. J.; Tao, A.; Law, M.; Fan, R.; Yang, P. *Adv. Mater. (Weinheim, Ger.)* **2007**, *19*, 61.
(6) Tong, L.; Lou, J.; Mazur, E. *Opt. Express* **2004**, *12*, 1025.
(7) Tong, L.; Gattass, R. R.; Ashcom, J. B.; He, S.; Lou, J.; Shen, M.; Maxwell, I.; Mazur, E. *Nature (London)* **2003**, *426*, 816.
(8) Snyder, W.; Love, J. D. *Optical waveguide theory*, 1st ed.; Chapman and Hall: London, 1983.
(9) Cadien, K. C.; Reshotko, M. R.; Block, B. A.; Bowen, A. M.; Kencke, D. L.; Davids, P. *Proc. SPIE* **2005**, *5730*, 133.
(10) Krauss, T. F. *Nat. Photonics* **2008**, *2*, 448.
(11) Mortensen, N. A.; Xiao, S. *Appl. Phys. Lett.* **2007**, *30*, 141108.
(12) Maslov, A. V.; Ning, C. Z. *Appl. Phys. Lett.* **2003**, *83*, 1237.
(13) Seo, M.-K.; Yang, J.-K.; Jeong, K.-Y.; Park, H.-G.; Qian, F.; Ee, H.-S.; No, Y.-S.; Lee, Y.-H. *Nano Lett.* **2008**, *8*, 4534–4538.
(14) Freude, W.; Hui-Hai, Y.; Zhi-Jian, H. *J. Lightwave Technol.* **1988**, *6*, 318.
(15) Houdré, R.; Weisbuch, C.; Stanley, R. P.; Oesterle, U.; Pellandini, P.; Ilegems, M. *Phys. Rev. Lett.* **1994**, *73*, 2043.
(16) Thévenaz, L. *Nat. Photonics* **2008**, *2*, 474.
(17) Vugt, L. K. v.; Rühle, S.; Vanmaekelbergh, D. *Nano Lett.* **2006**, *6*, 2707.
(18) Voss, T.; Thomas, G.; Svacha Mazur, E.; Mueller, S.; Ronning, C.; Konjhodzic, D.; Marlow, F. *Nano Lett.* **2007**, *7*, 3675.
(19) Lukin, M. D.; Imamoglu, A. *Phys. Rev. Lett.* **2000**, *84*, 1419.
(20) Philipose, U.; Saxena, A.; Ruda, H. E.; Simpson, P. J.; Wang, Y. Q.; Kavanagh, K. L. *Nanotechnology* **2008**, *19*, 215715.
(21) Kiselev, V. A.; Razbirin, B. S.; Uraltsev, I. N. *Phys. Status Solidi B* **1975**, *72*, 161.
(22) Adachi, S.; Taguchi, T. *Phys. Rev. B: Condens. Matter* **1991**, *43*, 9569.
(23) Hopfield, J. J. *Phys. Rev.* **1958**, *112*, 1555.
(24) Reithmaier, J. P.; Sek, G.; Löffler, A.; Hofmann, C.; Kuhn, S.; Reitzenstein, S.; Keldysh, L. V.; Kulakovskii, V. D.; Reinecke, T. L.; Forchel, A. *Nature (London)* **2004**, *432*, 197.
(25) Vugt, L. K. v.; Rühle, S.; Ravindran, P.; Gerritsen, H. C.; Kuipers, L.; Vanmaekelbergh, D. *Phys. Rev. Lett.* **2006**, *97*, 147401.

NL900371R